

PROBABILISTIC ANALYSIS OF RIGID BLOCK STABILITY

Martin Grenon, Mining, Metallurgical and Material Engineering, Université Laval, Canada.

John Hadjigeorgiou, Mining, Metallurgical and Material Engineering, Université Laval, Canada.

Frank Lemy, Geological Engineering, ETH Zurich, Switzerland.

ABSTRACT

This paper provides an integrated methodology that uses random fracture network generation techniques and individual rigid block stability analysis to fully capture the probability of occurrence and stability of wedges at the crest of a rock slope.

RÉSUMÉ

Cet article présente une approche intégrée combinant la génération de réseaux aléatoires de fracture et l'analyse de la stabilité des blocs rigides pour déterminer la probabilité d'occurrence et la stabilité des dièdres au sommet des pentes rocheuses.

1. INTRODUCTION

As early as 1972 Piteau argued convincingly that the "...stability of slopes in rock is determined principally by structural discontinuities in the mass and not by the strength of the rock itself". Piteau suggests that a prerequisite for a rational analysis of rock slopes is the reliable application of the following geological premises:

- The characteristics of the joint population (generic structural type, orientation and position in space, intensity, joint wall rock hardness and asperities, joint size, infilling and alteration materials between joint planes) can be determined. The description of the joint population should be based on a sampling basis with statistical analysis and judgment used to determine whether the best estimate is made of the whole population.
- Structural regions can be defined, with the implication that the joint population within a defined region displaying similar characteristics.
- A reliable model of the joints in the mass can be constructed. This implies that a statistical sampling of any property will give a representative picture of the entire portion of the rock mass it is meant to depict.
- Failure is confined to preexisting planes or combinations of planes. This implies that there are various modes of failure which are kinematically possible.

Rock slope failures are often classified into: planar, wedge, toppling and circular. It is the structural discontinuities in the rock mass that dictate the failure mechanism. This paper investigates rock slopes susceptible to wedge type failures.

Hoek and Bray (1981) provide the standard methodology for the stereographic interpretation of rock structure as well as general limit equilibrium for the analysis of wedge type failure in rock. Presently several computer software

are available that rely on limit equilibrium analysis to facilitate wedge type of analysis. The more advanced of these software are also capable of capturing the inherent variability in the mechanical properties and orientation of fractures in rock.

A shortcoming of most wedge analysis software packages is their inability to account for fracture location and frequency. This paper presents an integrated methodology whereby it is possible to generate random fracture networks and consequently investigate the stability of each defined wedge using a generalised limit equilibrium analysis. This provides a more representative analysis of rock slopes susceptible to wedge failure.

2. WEDGE ANALYSIS

Piteau (1972) has observed that the creation and occurrences of wedge type failures is controlled by the lithology and structure of the rock mass. The mechanics of a sliding wedge in a rock slope have been defined by Hoek and Bray (1981). The generalised geometry is presented in Figure 1, where the failure surfaces are denoted by 1 and 2, the upper ground surface by 3, the slope face by 4 and the tension crack (if present) by 5. H_1 is the slope height referred to plane 1.

The necessary conditions for wedge failure are defined in Figure 1 and Figure 2 whereby:

$$\psi_{fi} > \psi_i > \phi$$

where

- | | |
|-------------|---|
| ψ_{fi} | = inclination of the slope face |
| ψ_i | = dip of the line of intersection |
| ϕ | = angle of friction along the failure plane |

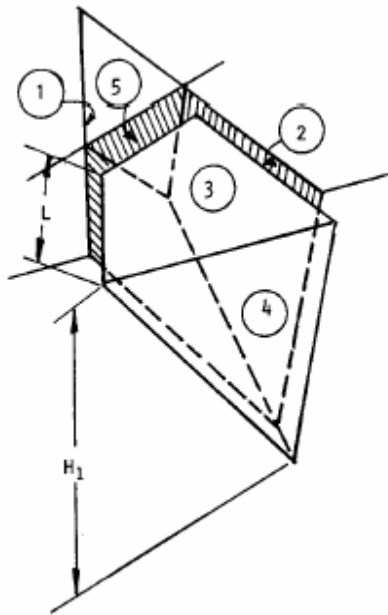


Figure 1. Typical wedge geometry: 1) & 2) intercepting fractures, 3) upper ground surface, 4) slope face, 5) tension crack, H_1 the slope height and L the distance of tension crack from crest (from Hoek & Bray 1981).

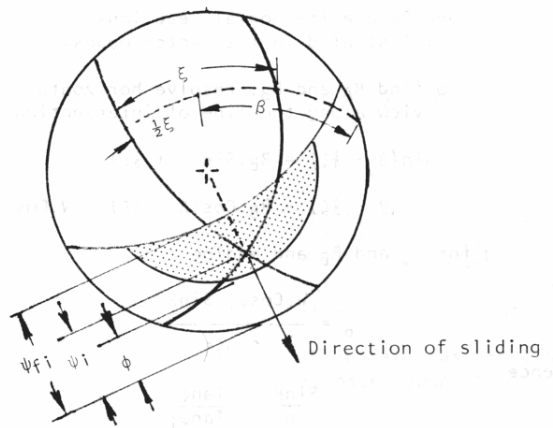


Figure 2. Stereographic representation of the necessary kinematic conditions for failure.

If the kinematic analysis suggests that the investigated fracture configuration can result in wedge failure a more detailed analysis, as proposed by Hoek and Bray (1981) is undertaken to determine the factor of safety, F :

$$F = \text{resisting forces/actuating forces}$$

A basic assumption is that the wedge behaves like a rigid body sliding along a plane, or along the intersection of two planes. As the sliding wedge does not undergo any

rotation, it follows that all acting forces pass through the centroid of the wedge.

A limitation of most current engineering analyses of wedge instability is the inability to account for fracture location, frequency and size distributions that in fact define all possible wedges. Fracture size controls the volume and extent of unstable wedges. If the spatial variability of the structural regime is not considered, i.e. fractures being considered ubiquitous, it is not possible to determine the probability of occurrence of a wedge. In traditional analyses this implies that all wedges have an equal probability to be present at a particular site. Obviously this is not necessarily true.

3. IRON ORE MINE

In order to demonstrate the integrated approach where a better representation of the structural regime of fractured rock masses is integrated to a limit equilibrium analysis an application is drawn from an iron ore mine at Koolan Island. The structural data have been collected by Priest & Samaniego (1988) for the hanging-wall slope of the mine. The rock type encountered is Arbitration cove quartzite and was heavily fractured. The data were further manipulated assuming that the sampling plane was oriented at 65/000 (dip/dip direction) and the sampling line at a trend 090 and a plunge of 00. This has allowed the determination of the fracture frequency along a line (P_{10}) as indicated in Table 1.

Table 1. Fracture characteristics for the hanging-wall slope (adapted from Priest & Samaniego 1988).

Set	Orient. (deg)	K	Trace (m)	P_{10}^* (m^{-1})	c kPa	ϕ (deg)
1	79/113	262	3.7	1.55	15	30
2	59/100	99	3.7	2.55	15	30
3	27/027	84	2.4	0.34	20	35
4	55/036	106	1.9	0.65	20	35
5	65/006	69	2.4	0.19	20	35
6	68/345	100	2.2	0.07	20	35
7	70/309	41	4.1	3.32	15	30
8	49/215	91	10	0.82	10	28

* calculated from original data

Fracture orientation is given by the mean dip and dip direction. The Fisher constant K is used to represent the dispersion of the orientation data around the mean value. The trace length is the length of the cord of a fracture intersecting the mining face. P_{10} is the fracture frequency along a line. The mechanical properties of rock fractures are defined by cohesion (c) and the angle of friction (ϕ) along the fracture.

4. FRACTURE SYSTEM MODELLING

There are several approaches of varying complexity to fracture system modelling. The basis for the developed fracture system generator used in this paper is the

Veneziano model described in Dershowitz & Einstein (1988). The model relies on the generation of a Poisson network of planes in 3D space followed by a secondary process of tessellation by a Poisson line process and marking of polygonal fractures. The Veneziano model is conceptually simple and the required input parameters can be easily inferred from field data.

The information in Table 1 was used to generate a three dimensional fracture system in a 25 x 25 x 25m volume, Figure 2. All generated fractures are of a polygonal shape. The generation is realised on a set basis, using as input fracture size, intensity, orientation, co-planarity and location data. Furthermore, the modified Veneziano model can consider discrete and stochastically located fractures. An interesting feature of the developed software is the potential to introduce several structural regimes in the generated volume.

In order to explore and quantify the significance of this approach the same input data were used to generate a series of three dimensional fracture systems of the same volume. In all 25 distinct fracture systems were generated.

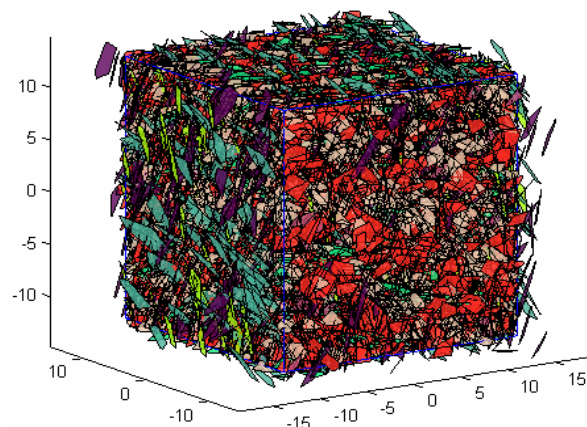


Figure 2. Fracture system from simulation #1.

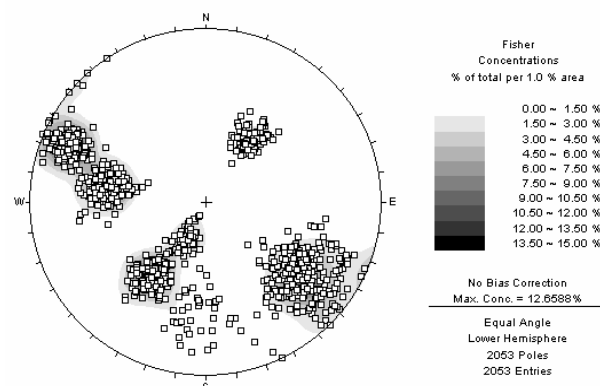


Figure 3. Stereonet from simulation #1.

Figure 3 and Table 1 present the characteristics of the first modelled fracture system. A virtual plane oriented at 65/000 was used to identify the exposed generated fractures. In all 2053 fractures were identified and grouped into 8 sets on the stereonet, Figure 3. It should be noted that the mean orientation and dispersion (K) for the fracture sets was statistically equivalent to the field data. There was some divergence on mean trace length and fracture frequency, but well within the limits of statistical similarity with the field data. The same fracture mechanical properties were used for all simulations. In all similar results were obtained for the other 24 other networks thus providing 25 equally probable in-situ fracture system representations for the hanging-wall slope of the mine.

Table 2. Generated fracture characteristics, simulation #1.

Set	Orient. (deg)	K	Trace (m)	P_{10} (m^{-1})	c (kPa)	ϕ (deg)
1	80/113	198	2.87	1.44	15	30
2	58/100	109	3.31	2.12	15	30
3	27/027	92	2.88	0.16	20	35
4	55/037	98	2.19	0.64	20	35
5	67/020	55	1.76	0.16	20	35
6	68/350	121	3.29	0.08	20	35
7	71/309	36	3.58	2.88	15	30
8	47/216	91	10	0.80	10	28

The inherent variability of equally probable fracture systems is illustrated in Figures 4 and 5. This variability is an outcome of the stochastic generation process where all generated systems are a possible representation of the in-situ conditions. The circles in Figure 2 represent the mean trace length values on a virtual plane oriented at 65/000 for all fracture sets. The sampled field values are represented by black squares and it is possible to quantify the variability with respect to the field values.

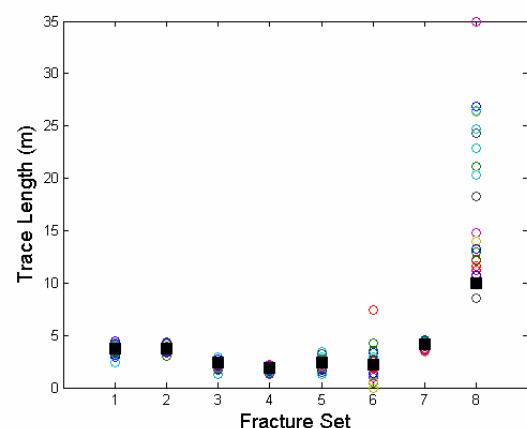


Figure 4. Variability of generated mean trace length.

In Figure 5 one can observe the same thing for fracture set frequency along a line (P_{10}) oriented at 090/00. The fracture system modelling tool is thus able to generate

probable representations of the in-situ structural conditions.

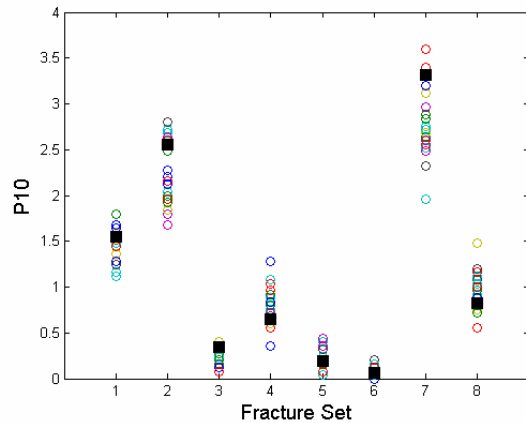


Figure 5. Variability of generated mean fracture frequency.

5. STABILITY ANALYSIS OF RIGID WEDGES

The stability of all wedges formed at the crest of a mining bench (10m high, 7m wide and 25m length along the crest) oriented at 65/000 was investigated. A limit equilibrium analysis was undertaken for all 25 generated random fracture systems.

In all 25 generated systems the crest of the slope was located in the centre of the generated rock mass. Along the length of the crest in the first system 207 fractures (36 from set #1; 53 from set #2; 4 from set #3; 16 from set #4; 4 from set #5; 2 from set #6; 72 from set #7 and 20 from set #8). The most dominant were fractures associated with sets #1, #2, and #7.

In section 2 it was noted that a wedge may form from the intersection of two fractures along the crest of a slope. The interest in the developed methodology lies in that it allows the representation and simultaneous analysis of all tetrahedral wedges. In fact as illustrated in Figure 6, 196 were formed based on simulation 1. The developed methodology has several other advantages. For example it is possible to identify the biggest wedge (in this simulation is 6.3 m^3) the total volume of wedges along the crest (60 m^3) and the number of wedges bigger than a selected threshold (for example 28 were larger than 0.1 m^3).

Another interesting information is the influence of each fracture set in defining feasible wedges. Figure 7 focuses at the 28 larger wedges. It is noted that fracture sets 2 and 7 are the two most prominent while sets 6 and 8 do not participate in the creation of any wedges along the crest.

The size distribution of wedges is more evident in Figure 8, focusing on the 28 largest wedges, where 4 wedges have a volume higher than 1 m^3 .

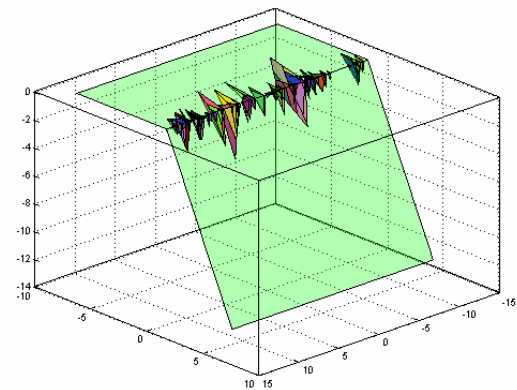


Figure 6. Tetrahedrons formed along the crest in simulation #1.

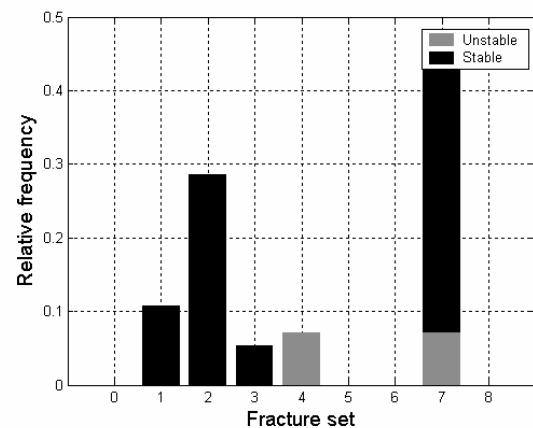


Figure 7. Fracture set contribution to wedge formation in simulation #1.

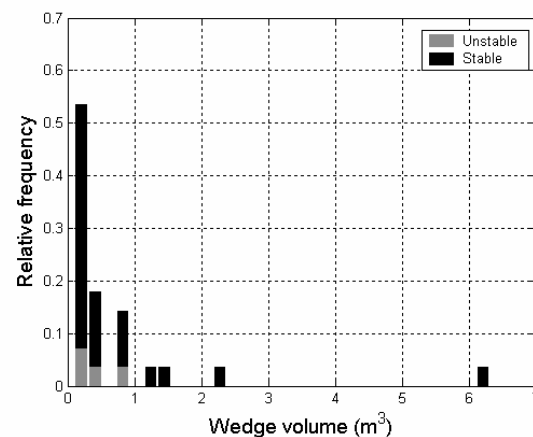


Figure 8. Wedge volume distribution in simulation #1.

This analysis assumes that wedge failure can be either by sliding along a plane or sliding along the line of intersection of both planes. In fact a kinematic analysis of all possible combinations has indicated that no sliding along a plane was possible for any of the 8 sets. Figure 9 is an abridged representation of all possible combinations of the different sets. For the purposes of clarity only the combinations that result in kinematically possible wedges are shown.

In fact all generated wedges, in this analysis, were susceptible to sliding along the line of intersection of two planes, Figure 9. For the 28 feasible wedges, it was fracture sets 2 and 7 that were most likely to form wedges.

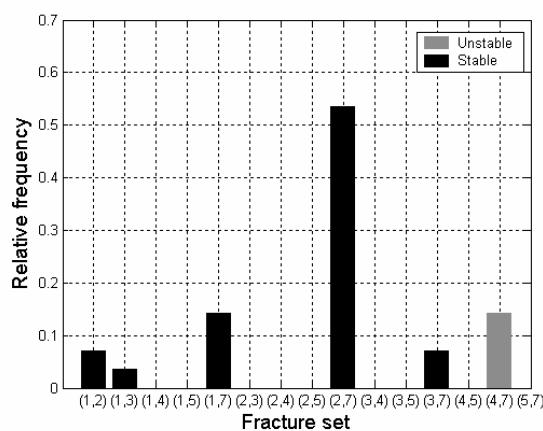


Figure 9. Potential mode of failure in simulation #1.

The Hoek and Bray (1981) methodology was used to assess the individual safety factor for all possible rigid wedges defined by two fracture sets. Figure 10 presents the cumulative pdf for the factor of safety of the 28 wedges along the crest studied in system 1. It can be observed that less than 13% of those wedges are unstable, i.e. factor of safety < 1. The cumulative pdf graph facilitates the use of site specific design criteria. If for example a threshold of a factor of safety of 1.5 is selected this would imply that the number of potentially unstable wedges would be 11, or 39% of all defined wedges.

Further information can be derived from Figures 7-9, where the proportion of unstable and the stable wedges is given. In particular it can be seen that fracture set that contribute to the creation of a number of wedges are in fact not critical to the stability of the excavation. On the other hand, wedges that tend to form along fracture set 4 tend to be unstable. Figure 8 clearly reveals that the volume of most unstable wedges in this analysis is not large. Figure 9, demonstrates clearly that sliding along the line of intersection of sets 4 and 7 is the only probable mode of failure for these conditions.

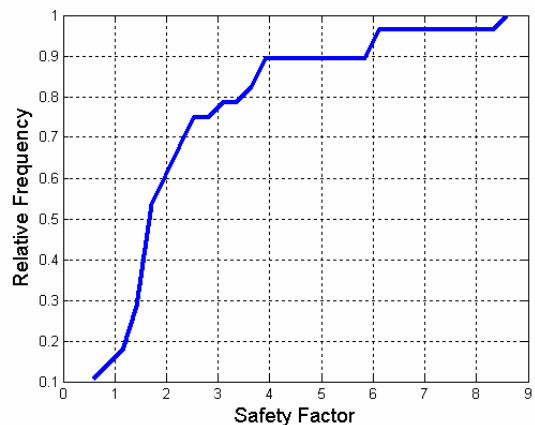


Figure 10. Cumulative PDF for the factor of safety in simulation #1.

There is no statistical correlation between wedge size and factor of safety. This is clearly illustrated on the scatter plot presented in Figure 11.

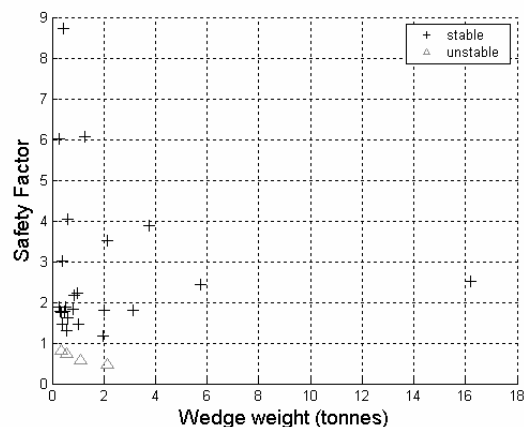


Figure 11. Scatter plot between wedge size and factor of safety in simulation #1.

As one might have expected, there is a strong correlation between the factor of safety and the plunge of the line of intersection of the two intersecting fractures that form a wedge, Figure 12.

The preceding analysis illustrated the advantages of using fracture systems to investigate the stability of rock slope susceptible to wedge failure. In fact the major advantage of the developed methodology lies in the potential to investigate several equally probable generated fracture networks. The 25 generated fracture systems all have an equal chance of representing the fracture distribution in-situ. Consequently, it can be argued that an analysis of the 25 fracture systems will best capture the rock mass and provide more instructive indication on the stability of the excavation.

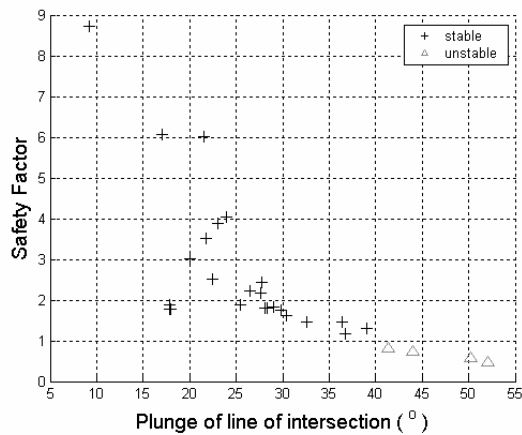


Figure 12. Scatter plot between the factor of safety and plunge line of intersection in simulation #1.

It is necessary to establish how many simulations should be run prior to accepting the validity of results. This is obviously influenced by the importance of the problem, the repercussions of failure, time constraints etc. Another way of presenting this dilemma is to decide at which point in the analysis it is assumed that the worst case scenario has been established. In the present case, due to time constraints, 25 realisations were arbitrarily chosen to expose the proposed methodology.

The total wedge volume along the crest varies between 4.5 and 32 m³, figure 13. Figure 14 presents the histogram for maximum unstable wedge. If the intention is to establish the largest possible unstable wedge at the crest of the studied slope then this is less than 2.5 m³.

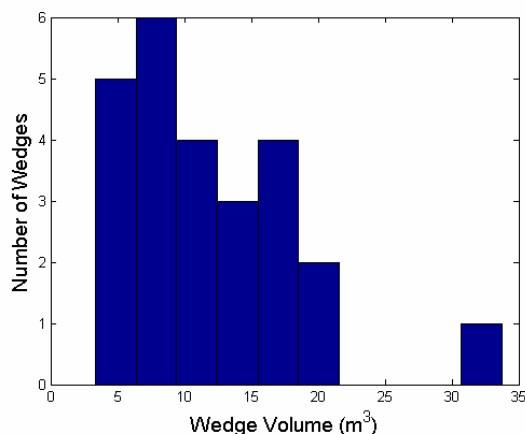


Figure 13. Total wedge volume distribution for 25 simulations.

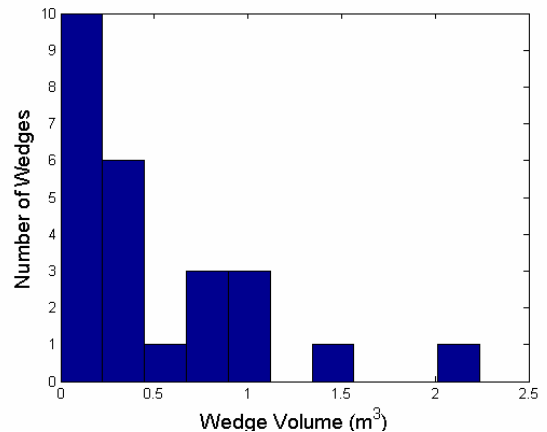


Figure 14. Maximal unstable wedge volume distribution for 25 simulations.

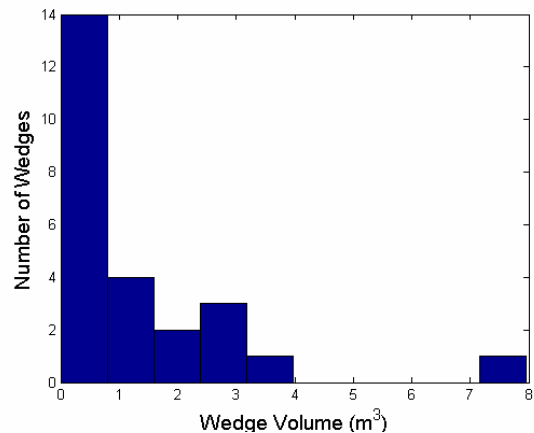


Figure 15. Total unstable wedge volume distribution for 25 simulations.

Figure 15 presents the histogram for total unstable wedge volume at the crest of the studied slope. Despite some variability in the results it can be argued that the maximal volume is 8 m³ along a 25 m crest. This type of analysis provides a mean of quantifying the probability of occurrence and the reliability of a given design.

6. CONCLUSIONS

This paper has provided an integrated methodology that uses random fracture network generation techniques and individual rigid block stability analysis to fully capture the probability of occurrence and stability of wedges at the crest of a rock slope.

This approach enables for specific in-situ fracture conditions and slope geometries to assess the critical parameters for stability issues. The most critical fracture sets combination, the probability of occurrence of wedges

type and size, the maximal wedge size and the total unstable volume may be assessed.

To address the risk associated with a given design the consequences of wedge instabilities must be accounted for. These consequences may be equipment loss or lost production and can have major economical impacts on the viability of a project.

Acknowledgements

The authors would like to acknowledge the financial contributions of the *Fonds Québécois de la Recherche sur la Nature et les Technologies* and the *Natural Sciences and Engineering Research Council of Canada*.

References

- Hoek E. & Bray J.W. 1977. Rock slope engineering. The Institution of Mining and Metallurgy, London, p. 402.
- Dershowitz, W. S. & Einstein, H. H. 1988. Characterizing rock joint geometry with joint system models. *Rock mechanics and rock engineering* volume 21, pp. 21-51.
- Piteau D.R. 1972. Engineering Geology Considerations and Approach in Assessing the Stability of rock Slopes. Bulletin of the Association of Engineering Geologists. Vol. IX, No.3, pp 301-320.
- Priest, S.D. & Samaniego, J.A. 1988 Face stability analysis in fractured rock by the statistical simulation of rigid block failure Proceedings of the 5th Australia-New Zealand conference on Geomechanics, The Institution of Engineers Australia, Sydney, pp. 398-403.